

## Photo-stability and Photo-reactivity of halogenated 8-methoxypsoralen, the basis for designing of new drugs

Klefah A.K. Musa<sup>1,\*</sup>, Salama Omar<sup>2</sup> and L. A. Eriksson<sup>3</sup>

1. Department of Medicinal Chemistry, Pharmacy College, El-mergib University, Al-khoms, Libya.
2. Department of Applied Physical Chemistry, Chemical Engineering Section, Faculty of Sciences, Autonoma University-Madrid, 28 049, Spain
3. Department of Chemistry and Molecular Biology, Göteborg University, SE 405 30 Göteborg, Göteborg, Sweden.

### ABSTRACT

8-methoxypsoralen is an efficient photosensitizer agent, used widely in PUVA therapy in treatment of different skin disorders like psoriasis, and other inflammatory skin disorders or recently in treatment of cancer diseases such as cutaneous T-cell lymphoma. Teen different substitutions of this compound have been made in this work, through fluorine and bromine atoms substitutions in order to increase its photosensitizer efficiency. In each system, we replace only one hydrogen atom of 8-methoxypsoralen by fluorine atom in the first five system, whereas, in the other five system substituted made by bromine atoms. These teen systems are studied by means of computational quantum method-DFT at MPWB95/6-311+G(d,p) level of theory. The results show that the 3-bromo-8-methoxypsoralen (X<sub>5</sub> system; of bromine substituted case) has the smallest transition state energy among all suggested teen compounds with a barrier accounted only 2.92 kcal/mol. Optimization of the neutral, radical anion and radical cation, triplet state, electron affinity, ionization potential, transition state energy, defluorination or debromination process of each system is obtained and discussed in detail.

**Key words:** DFT, photosensitization, psoralen, 8MOP.

### Introduction

Psoralens or furanocoumarins are well known since a long time ago as photosensitizers and later on, they introduced to the medical field, to be used in photodynamic drug therapy. Since, they react with appropriate wavelengths (UVA) of spectrum of the light irradiation and known as PUVA therapy [1]. Several studies have been made to understand the properties of this type of drug families, going from their synthesis to investigate their pharmacological action and side effects of the parent psoralen compounds or their derivatives such as benzopsoralen [1, 2]. Previous study reported that the introduction of a benzene ring fused to the furan, or the addition of bulky or electron withdrawing substituents into the pyrone ring are suggested as potential ways of inhibiting adduct formation with DNA [3], the another studies concluded that the possibility of diadducts formation with DNA is responsible for unwanted side effects [1, 4]. The introduction of an ester group into a benzopsoralen can provide derivatives which are work as efficient photosensitizers yielding singlet oxygen [2],

whereas the presence of one or more methyl groups in psoralen analogues angelicin, increase their photobinding ability to DNA [4]. *In vitro* study shows that the psoralens derivative found to be active against human melanoma cell line [5].

Because of the UV light absorbing properties of psoralens and bergapten, they used in pharmaceutical and cosmetic products. Their usage increased in dermatology as the photochemotherapeutic agents to treat a variety of diseases such as vitiligo, psoriasis, mycosis fungoides, atopic eczema and alopecia [6-7].

Furthermore, the use of psoralens in medicine has been associated with higher incidence of skin cancer [8-10]. In this sense, several studies have been demonstrated that the psoralen are able to cause phototoxicity side effects and considered as carcinogenic, mutagenic and photodermatitic agents [11-13]. These drugs are photoreactive with nucleic acids especially when irradiated with long wavelengths of

the ultraviolet light (320-400 nm); (UVA). Due to they can form covalent cross-links with DNA base paired structures, they are unique in their ability to freeze helical region of nucleic acids. Thus, they have been extensively used to probe the higher-ordered nucleic acid structures [14]. PUVA (psoralen with UVA therapy) appears to have a steroid-sparing effect and immunomodulatory effects, thus in turn used to treat a variety of immune-mediated dermatological diseases [15].

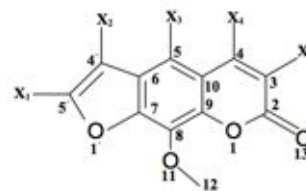
Photochemotherapy employing 8-methoxypsoralen (8MOP) and UVA irradiation (PUVA) is widely used in the treatment of different skin disorders like psoriasis, T-cell lymphoma and other inflammatory skin disorders. Psoralens in general are tricyclic aromatic structures act as photosensitizers providing reactive oxygen species such as singlet oxygen and superoxide radical anion. These agents facilitate their intercalation with DNA base pairs upon photo-excitation because of their planer structures [16], e.g., resulting in the formation of photoadducts with pyrimidines in cellular DNA which believed to be the primary cause of photoinduced cell killing. In addition to their cause to oxidative damage, they generate mono- and di-adducts leading to DNA inter-strand cross-links with increased chromosome breakage and DNA fragmentation [17]. New psoralen derivatives such as angelicin that is an angular psoralen which allows only monofunctional photobinding thus reducing undesirable side effects, especially long term ones such as genotoxicity and risk of skin cancer [4].

Recently, 8MOP is approved for clinical application of extracorporeal photo-chemotherapy (ECP) which is a therapeutic approach based on the photo-biological effects of 8-MOP on white blood cells isolated from patient blood and exposed to UVA prior to reinfusion. This treatment used in cutaneous T-cell lymphoma, systemic sclerosis, graft-versus-host disease, and in the organ rejection [18-20].

Oral administration of 8-MOP is easy to accomplish and inexpensive but oral PUVA therapy is associated with a variety of potential side effects caused using the systemic administration of the drug [21-23]. These side effects may limit the long-term use of oral PUVA therapy for some patients. Topical PUVA therapy using bath or cream is an alternative treatment which is as effective as oral PUVA therapy [24-27]. Using topical medications, the drug concentrations on the skin might be even higher than in case of oral administrations and less side effects because the systemic availability of topical applied 8-MOP is limited [28, 29].

In order to provide another photosensitizer form of 8MOP with higher reactivity, we in the present work, studied teen different systems<sup>†</sup>, in each system we substituted only one

hydrogen atom of 8MOP by either F and Br atom at determined position. For instance, in X<sub>1</sub> system we substituted the hydrogen atom at position X<sub>1</sub> by either F or Br atom. In Figure 1, we show the chemical structure of 8MOP and its possible different substitutions forming the teen systems studied in this context.



†The teen systems are as follows:

In case fluorine substitution (X=F).	In case of bromine substitution (X=Br).
X <sub>1</sub> system : 5'-fluoro-8-methoxypsoralen.	X <sub>1</sub> system : 5'-bromo-8-methoxypsoralen.
X <sub>2</sub> system : 4'-fluoro-8-methoxypsoralen.	X <sub>2</sub> system : 4'-bromo-8-methoxypsoralen.
X <sub>3</sub> system : 5-fluoro-8-methoxypsoralen.	X <sub>3</sub> system : 5-bromo-8-methoxypsoralen.
X <sub>4</sub> system : 4-fluoro-8-methoxypsoralen.	X <sub>4</sub> system : 4-bromo-8-methoxypsoralen.
X <sub>5</sub> system : 3-fluoro-8-methoxypsoralen.	X <sub>5</sub> system : 3-bromo-8-methoxypsoralen.

Figure 1. Scheme representation of 8-MOP substitutions at different X positions (by either F or Br).

## Methodology

All 10 different system geometries were optimized, in their neutral, anionic, cationic, triplet, transition state, and product at the MPWB95/6-311+G(d,p) level of theory [30]. Single-point calculations were performed on these geometries utilizing the same bases set and level of theory. Solvent effects were taken into consideration implicitly, through single point calculations on the optimized geometries at the same level of theory, including the integral equation formulation of the polarized continuum model (IEFPCM) [31-33]. Water was used as solvent, through the value 78.31 for the dielectric constant in the IEFPCM calculations. The vertical electron affinity (VEA) (ionization potential, VIP) is calculated as the energy difference between the neutral species and the anionic (cationic) species at the geometry of the neutral molecule. Frequency calculations were performed on the optimized geometries at the same level of theory, to ensure the systems to be local minima (no imaginary vibrational frequencies except for transition state optimizations), and to extract zero-point vibrational energies (ZPE) and thermal corrections to the Gibbs free energies at 298 K. The numbering scheme of the atoms used throughout the study is given in Figure 1. All calculations were performed with the GAUSSIAN 03 programme package [34].

## Results and discussion

### I- Fluorine substitution.

We studied five systems of fluorine substitution at different positions in 8MOP molecule. In each system we substituted only one fluorine atom at one of these positions (5', 4', 5, 4

or 3) of 8MOP as they manifested in the figure-1. The main important optimized feature is the bond which connects the halogen atom (F) and the carbon atom in the structure of 8-MOP. The Table 1 shows this feature for all systems studied and their singlet, anion, cation, triplet and transition state. For all system studied herein, the C-F bond length is increased (decreased) by about 0.02 Å in anion (cation) species compared with the corresponding neutral forms, and no much change in their corresponding triplets. However, in transition states, this bond length distance is decreased in the series order  $X_3 > X_4 > X_1 > X_5 > X_2$ .

Table 1. The gas phase optimized C-F bond lengths of the substituted 8-MOP systems, in Å.

system	The optimized C-F bond length				
	S <sub>0</sub>	anion form	cation form	T <sub>1</sub>	TS
X <sub>1</sub>	1.3	1.3	1.2	1.2	2.8
X <sub>2</sub>	1.3	1.3	1.3	1.3	2.0
X <sub>3</sub>	1.3	1.3	1.3	1.3	3.2
X <sub>4</sub>	1.3	1.3	1.3	1.3	3.0
X <sub>5</sub>	1.3	1.3	1.3	1.3	2.6

Table S1 and S2 in the supplementary material show the Mulliken atomic charges and unpaired spin densities distribution for selected atoms of the substituted 8MOP system molecules. Showing that the most negative charge is located at C9 in all species whereas the most positive charge is located at C10 for all species, as well as the C7 and C8 have less relative negative charge than C9 for all species. On the other hand, the unpaired spin density distribution for all systems show that the main spin densities for all systems is located at C5. The O13 in the system X4 and C7 in the system X5 have no significant spin densities if they compared with the same atoms for other systems.

In order to investigate the stability or the reactivity of these systems under theoretical study point of view; the relative

Gibbs free energies, electron affinity (EA), ionization potential (IP) and the energy gaps between the singlet and the triplet states of all system are calculated in solvent phase by IEFPCM methodology under the same level of theory explored in Table 2. The most stable system among all these systems under inclusion of bulk solvation effect is X4 system while the most unstable under the case situation is X2 system. Although, the energy difference among all systems is in range of 8 kcal/mol, the stability of these systems can be ranked in increased along the series  $X_2 < X_5 < X_3 < X_1 < X_4$ .

The redox-chemistry of these five systems investigated by calculation their electron affinity and ionization potential in solvent phase. The former is calculated by subtraction of the anion species energies from corresponding neutral forms energies. The computed differences in EA of these systems are in within 2 kcal/mol. On the other hand, the IP calculated by subtraction of neutral forms energies from corresponding energies of their cation species. Again, the computed energy differences in IP among all these systems are in range of 2.5 kcal/mol. The IP increases according to this series  $X_1 < X_3 < X_5 < X_4 < X_2$ , while EA decreases along this order  $X_3 > X_5 > X_2 > X_4 > X_1$ , indicating that the X1 has the lowest EA and IP energies among all systems, the easiest to oxidized and reduced, so it is the most reactive species.

The singlet-triplet energy gaps of all the fluorine substituted systems are calculated and explored in Table 4. The lowest S<sub>0</sub>-T<sub>1</sub> energy gap is accounted for the X3 system, while the highest computed for X1 system. In general, the T<sub>1</sub> of all systems located high enough for the generation of singlet oxygen species. Since, the generation of singlet oxygen species from the ground state molecular oxygen natural required only 22.5 kcal/mol [35], while all systems provided T<sub>1</sub> states at around 56 kcal/mol, indicating possibility of this reactive oxygen species to formed once any system of them excited to its first excited triplet state.

Table 2. The absolute and the relative Gibbs free energies in kcal/mol, the electron affinity, the ionization potential and the singlet-triplet gaps for fluorine substitution systems at MPWB95/6-311+G(d,p) level (in kcal/mol).

system	ΔG	ΔΔ G	EA	IP	Δ(S→T)
X <sub>1</sub>	-861.991626	0.0	60.65	133.67	56.64
X <sub>2</sub>	-861.983943	4.82	61.76	135.99	56.03
X <sub>3</sub>	-861.991056	0.36	62.86	133.86	53.98
X <sub>4</sub>	-861.995930	-2.70	61.45	135.76	56.17
X <sub>5</sub>	-861.989455	1.36	62.72	135.70	55.61

Defluorination process for each system of above mentioned systems studied by scanning the C-F bond length from the corresponding obtained optimized bond length in 0.1 Å steps. The transition state energy of each system calculated and displayed in Figure 2 and its corresponding TS distance measured and shown in Table 1. In this context, the relative energies are computed for transition states and their

products considering energies of reactants as zero. The smallest transition state energy is accounted for system X<sub>4</sub>, which equals 17.60 kcal/mol forming dissociated products at 11.06 kcal/mol. Indicating that the defluorination process occurs more easier than other systems, thus in turn, X<sub>4</sub> system is the most reactive system and expected to gives its action more efficient compared with other systems. The

most stable system among all fluorine substitution system having the highest TS energy at 21.73 kcal/mol with its products formed at 16.31 kcal/mol is X<sub>1</sub> system. Obviously, according to energy barriers of the defluorination processes of all system

clarified in Figure 2, the relative transition state energies are decreased in this order X<sub>1</sub> > X<sub>5</sub> > X<sub>3</sub> > X<sub>2</sub> > X<sub>4</sub>.

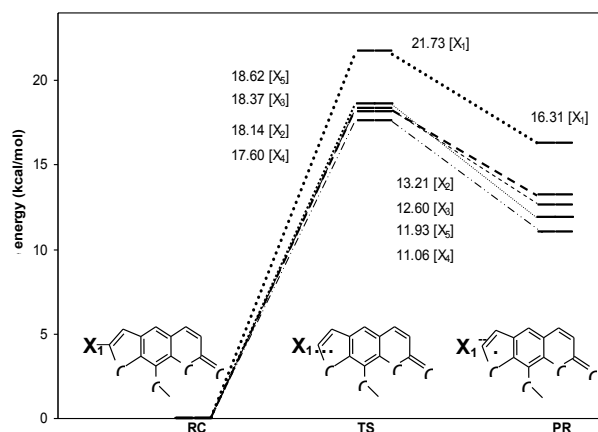


Figure 2. Defluorination energy barriers for all fluorine substitution systems, energies of reactants, TS, and products of each system is shown and one example for chemical structures is shown for X<sub>1</sub> system.

## II- Bromine substitution .

Five systems of 8MOP bromine substitution similar to that above mentioned with fluorine substitutions are studied under the same method and the level of theory.

As natural feature the optimized C-Br bond length of each system is longer system in the singlet, the radical anion and cation, the triplet state and the The main optimized features is the C-Br

bond length of each transition state are displayed in Table 3. than the corresponding C-F bond length by about 0.5 Å explained as halogen atom sizes. Similar with fluorine case, in all system studied with bromine substitutions, the C-Br bond length increase (decreased) by ~0.02 Å in the corresponding radical anion (cation) compared with the corresponding neutral species, again similar with fluorine case, no much change in the corresponding optimized triplet states. However, in the optimized transition states of the systems, herein different from fluorine case, the smallest C-Br bond length found in the X<sub>1</sub> system, which measured 2.04 Å, while the longest noted for the X<sub>5</sub> system. The TS for all systems are increased in this series X<sub>1</sub> < X<sub>2</sub> < X<sub>3</sub> < X<sub>4</sub> < X<sub>5</sub>.

Mulliken atomic charges distribution and the unpaired spin densities of selected atoms for all systems of bromine substitution are shown in supplementary materials in Table S3 and S4, respectively. The most negative charge for all

systems is condensed on C<sub>9</sub> while the most positive charge is located on C<sub>10</sub> with little differences among the systems. For the X<sub>1</sub> system, the charge are centered on C<sub>7</sub> while for the X<sub>2</sub> system, the charge is located more on C<sub>6</sub>. Whereas, the system X<sub>3</sub> and X<sub>4</sub> the charge are centered at C<sub>5</sub> and C<sub>4</sub> atoms, respectively. On the other hand, the main unpaired spin density for all systems is found at C<sub>5</sub>. In the system X<sub>3</sub> there is no significant unpaired spin density at O<sub>1</sub> compared with the corresponding atom in other systems. Transition states of different systems show that the unpaired spin densities are distributed between two main atoms, the bromine and the formerly connected carbon of each system. At transition states, the X<sub>5</sub> system has the highest unpaired spin densities at C<sub>3</sub> which formerly connected to bromine atom compared with other system.

Similar to the fluorine case and in order to investigate the stability or the reactivity of these systems under theoretical study point of view; the relative Gibbs free energies, electron affinity (EA), ionization potential (IP) and the energy gaps between the singlet and the triplet states of all system are calculated in solvent phase by IEFPCM methodology under the same level of theory explored in Table 4. The most stable system among all these systems under inclusion of bulk salvation effect is X<sub>4</sub> system (similar to fluorine case) while the most unstable under the case spin densities at C<sub>3</sub> which formerly connected to bromine atom compared with other system. Similar to the fluorine case and in order to investigate the stability or the reactivity of these systems under theoretical study point of view; the relative Gibbs free energies, electron affinity (EA), ionization potential (IP) and the energy gaps between the singlet and the triplet states of all system are calculated in solvent phase by IEFPCM methodology under the same level of theory explored in Table 4. The most stable system among all these systems under inclusion of bulk salvation effect is X<sub>4</sub> system (similar to fluorine case) while the most unstable under the case situation is X<sub>1</sub> system (unlike fluorine substitution case, it was X<sub>2</sub> system). Although, the energy difference among all systems is in range of 2 kcal/mol, the stability of these systems can be ranked in increased along the series X<sub>1</sub> < X<sub>2</sub> < X<sub>5</sub> < X<sub>3</sub> < X<sub>4</sub>. The redox-chemistry of these five systems also investigated by calculation their electron affinity and ionization potential in solvent phase. The computed differences in EA of these systems are in within 5 kcal/mol. On the other hand, the computed energy differences in IP among all these systems are in range of 2 kcal/mol. The IP decreases according to this series X<sub>4</sub> > X<sub>2</sub> > X<sub>5</sub> > X<sub>1</sub> > X<sub>3</sub>, while EA increases along this order X<sub>4</sub> < X<sub>5</sub> < X<sub>3</sub> < X<sub>2</sub> < X<sub>1</sub>, indicating that the X<sub>4</sub> has the highest EA and IP energies among all systems, the most difficult to oxidized and reduced, so it is the less reactive species (opposite to X<sub>1</sub> system, in case of fluorine substitutions).

Table 3. The gas phase optimized C-Br bond lengths of the substituted 8MOP systems, in Å.

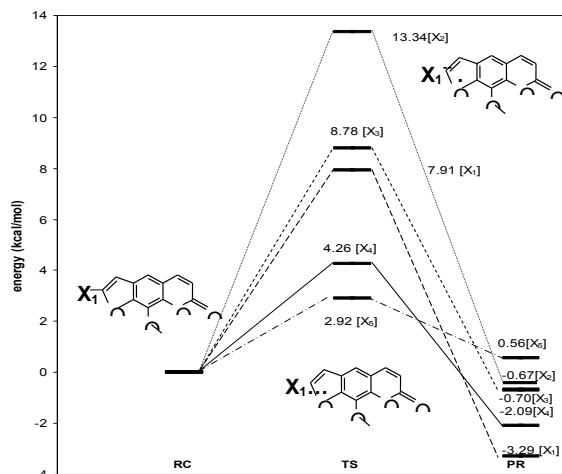
system	The optimized C-Br bond length				
	S <sub>0</sub>	anion form	cation form	T <sub>1</sub>	TS
X <sub>1</sub>	1.848	1.862	1.823	1.842	2.040
X <sub>2</sub>	1.860	1.873	1.843	1.858	2.145
X <sub>3</sub>	1.885	1.897	1.849	1.856	2.170
X <sub>4</sub>	1.885	1.903	1.866	1.886	2.244
X <sub>5</sub>	1.871	1.895	1.856	1.837	2.473

Table 4. The absolute and the relative Gibbs free energies in kcal/mol, the electron affinity, the ionization potential and the singlet-triplet gaps for bromine substitution systems at MPWB95/6-311+G(d,p) level (in kcal/mol).

system	ΔG	ΔΔG	EA	IP	Δ(S→T)
X <sub>1</sub>	-3336.636365	0.0	61.25	134.71	56.46
X <sub>2</sub>	-3336.636555	-0.12	61.61	135.79	56.21
X <sub>3</sub>	-3336.637943	-0.99	64.67	134.26	52.35
X <sub>4</sub>	-3336.639211	-1.79	65.32	135.82	53.14
X <sub>5</sub>	-3336.637448	-0.68	64.79	135.41	55.97

The singlet-triplet energy gaps of all the bromine substituted systems are calculated and explored in Table 4. The lowest S<sub>0</sub>-T<sub>1</sub> energy gap is accounted for the X<sub>3</sub> system (52.35 kcal/mol), (similar to fluorine substitution systems case), while the highest computed for X<sub>1</sub> system (56.46 kcal/mol). Again, as general for all systems studied

herein, the T<sub>1</sub> of all systems located high enough for the generation of singlet oxygen species. Indicating possibility of this reactive oxygen species to formed once any system of them excited to its first excited triplet state, i.e. the bromine substituted 8MOP expected to work efficiently in generation of singlet oxygen and thus giving its pharmacological action.



**Figure-3.** Relative energy curve shows the different transition states and their products for five systems in case of bromine substitution. There is an example for chemical structures of reactant, transition state and product for system X<sub>1</sub> and by similar way for other systems.

Debromination process for each system of above mentioned systems studied by scanning the C-Br bond length from the corresponding obtained optimized bond length in 0.1 Å steps. The transition state energy of each system calculated and displayed in Figure 3 and its corresponding TS distance measured and shown in Table 3. In this context, the energies are computed for transition states and their products considering energies of reactants as zero. The smallest transition state energy is accounted only 2.92 kcal/mol for system X<sub>5</sub>, forming dissociated products at 0.56 kcal/mol. Indicating that the debromination process occurs more easier than other systems, thus in turn, X<sub>5</sub> system is the most reactive system and expected to gives its action more efficient compared with other systems. The most stable system among all bromine substitution system having the highest TS energy at 13.34 kcal/mol with its products formed at -0.67 kcal/mol is X<sub>2</sub> system. Obviously, according to energy barriers of the debromination processes of all system clarified in Figure 2, the transition state energies are increased in this order X<sub>5</sub> < X<sub>4</sub> < X<sub>1</sub> < X<sub>3</sub> < X<sub>2</sub>.

In general, the debromination process from any of the substituted 8MOP system very easier than the defluorination process of any of the substituted 8MOP system, where the highest energy barrier of the defluorination of the fluorinated 8MOP system is lesser than the lowest energy barrier of the debromination of brominated 8MOP system. Indicating that the debromination process occurs of any brominated 8MOP system more efficient than the corresponding defluorination process of any fluorinated 8MOP system.

### Conclusion

8-MOP is an efficient photosensitizer agent, used widely in PUVA therapy in treatment of different skin disorders like psoriasis, and other inflammatory skin disorders or recently in treatment of cancer diseases such as cutaneous T-cell lymphoma, and also used in organ rejection. In order to increase its photosensitizer efficiency by substitution with fluorine and bromine atoms, teen compounds are obtained, in each system, we replace only one hydrogen atom of 8MOP by fluorine atom in the first five system, whereas, the other five system substituted with bromine atom. These teen systems are studied by means of computational quantum method-DFT at MPWB95/6-311+G(d,p) level of theory.

The triplet states energies obtained for the teen molecules are around 65 kcal/mol, which are high enough for the generation of reactive oxygen species especially singlet oxygen, which naturally formed from molecular oxygen with  $\Delta E$  equal  $\sim 22.5$  kcal/mol.

The defluorination and the debromination energy barrier for each suggested system is obtained through the scan of the C-F and the C-Br bond length from their optimized bond length, respectively, in 0.1 Å steps. The transition state energies of all teen systems show that (i) the 3-bromo-8-methoxypsoralen (X<sub>5</sub> system; of bromine substituted case) has the smallest transition state energy among all suggested teen compounds with a barrier accounted only 2.92 kcal/mol. (ii) the lowest transition state energy of the substituted fluorine molecules is accounted for 4-fluoro-8-methoxypsoralen and computed to be at 17.60 kcal/mol. (iii) in general, the debromination process from any of the substituted 8MOP system very easier than the defluorination process of any of the substituted 8MOP system, where the highest energy barrier of the defluorination of the fluorinated 8MOP system is lesser than the lowest energy barrier of the debromination of the brominated 8MOP system.

### Acknowledgements

Department of Medicinal chemistry, Pharmacy College, El-mergib University, Al-khoms, Libya (KAKM), the Swedish Science Research Council and Department of Chemistry and Molecular Biology, Göteborg University, Göteborg, Sweden (LAE) and Faculty of Science at Auotonoma

University-Madrid (SO) are gratefully acknowledged for financial support. We also acknowledge generous grants of computing time at the National Supercomputing Center (NSC) in Linköping.

### References

- [1] Chilin, A.; Marzano, C.; Guiotto, A.; Manzini, P.; Baccichetti, F.; Carlassare, F. and Bordin, F., Synthesis and biological activity of (hydroxymethyl)- and (diethylaminomethyl) benzopsoralens., *J. Med. Chem.* **1999**, 42, 2936-2945.
- [2] Mobilio, S.; Tondelli, L.; Capobianco, M.; and Gia, O., Sequence specificity of tetrahydrobenzopsoralen photobinding to DNA, *J. Photochem. Photobiol.* **1995**, 61, 113-117.
- [3] Gia, O.; Mobilio, S.; Palumbo, M.; and Pathak, M. A., Benzo- and tetrahydrobenzo-psoralen congeners: DNA binding and photobiological properties, *J. Photochem. Photobiol.* **1993**, 57, 497-503.
- [4] Bordin, F.; Dallacqua, F.; and Guiotto, A., Angelicins, angular analogues of psoralens chemistry, photochemical photobiological and photochemotherapeutic properties. *Pharmacol. Ther.* **1991**, 52, 331-363.
- [5] Leite, V. C.; Santos, R. F.; Chen, L. C.; and Guillo, L. A., Psoralen derivatives and longwave ultraviolet irradiation are active in vitro against human melanoma cell line, *J. Photochem. Photobiol. B-Biol.* **2004**, 76, 49-53.
- [6] Jarvenpaa, E. P.; Jestoi, M. N.; and Huopalahti, R., Quantitative determination of phototoxic furocoumarins in celeriac (*Apium graveolens* L. var. *rapeceum*) using supercritical fluid extraction and high performance liquid chromatography, *Phytochem. Anal.* **1997**, 8, 250-256.
- [7] Bettero, A.; and Benassi, C. A., Determination of bergapten and citropten in perfumes and suntan cosmetics by high-performance liquid chromatography and fluorescence, *Journal of Chromatography* **1983**, 280, 167-171.
- [8] Chimichi, S.; Boccalini, M.; Cosimelli, B.; Viola, G.; Vedaldi, D.; and Dallacqua, F., A convenient synthesis of psoralens, *Tetrahedron* **2002**, 58, 4859-4863.
- [9] Nigg, H. N.; Strandberg, J. O.; Beier, R. C.; Petersen, H. D.; and Harrison, J. M., Furanocoumarins in Florida celery varieties increased by fungicide treatment, *J. Agric. Food Chem.* **1997**, 45, 1430-1436.
- [10] Kreimer-Erlacher, H.; Seidl, H.; Back, B.; Cerroni, L.; Kerl, H.; and Wolf, P., High Frequency of Ultraviolet Mutations at the INK4a-ARF Locus in Squamous Cell Carcinomas from Psoralen-Plus-Ultraviolet-A-Treated Psoriasis Patients, *J. Invest. Dermatol.* **2003**, 120, 676-682.
- [11] Vilegas, J. H. Y.; Lancas, F. M.; Vilegas, W.; and Pozzetti, G. L., Further triterpenes, steroids and furocoumarins from brazilian medicinal plants of

- dorstenia genus (moraceae), *J. Braz. Chem. Soc.* **1997**, 8, 529-535.
- [12] Franke, K.; Porzel, A.; Masaoud, M.; Adam, G.; and Schmidt, J., Furanocoumarins from *Dorstenia gigas*, *Phytochemistry* **2001**, 56, 611-621.
- [13] Dercks, W.; Trumble, J.; and Winter, C., Impact of atmospheric pollution on linear furanocoumarin content in celery, *J. Chem. Ecol.* **1990**, 16, 443-454.
- [14] Isaacs, S. T.; Shen, C. J.; Hearst, J. E.; and Rapoport, H., Synthesis and characterization of new psoralen derivatives with superior photoreactivity with DNA and RNA, *Biochemistry* **1977**, 16, 1058-1064.
- [15] Furlong, T.; Leisenring, W.; Storb, R.; Anasetti, C.; Appelbaum, F. R.; Carpenter, P. A.; Deeg, H. J.; Doney, K.; Kiem, H. P.; Nash, R. A.; Sanders, J. E.; Witherspoon, R.; Thompson, D.; and Martin, P., Psoralen and ultraviolet A irradiation (PUVA) as therapy for steroid-resistant cutaneous acute graft-versus-host disease, *J. Biol. Blood Marrow Transplant.* **2002**, 8, 206-212.
- [16] Gasparro, F. P.; Liao, B.; Foley, P. J.; Wang, X. M.; and McNiff, J. M., Psoralen Photochemotherapy, Clinical Efficacy, and Photomutagenicity: The Role of Molecular Epidemiology in Minimizing Risks, *Environ. Mol. Mutagen.* **1998**, 31, 105-112.
- [17] Omar, A.; Wiesmann, U. N.; and Krebs, A., Polyploidization and hemiplodization induced by PUVA in vivo, *Dermatologica* **1979**, 159, 195-209.
- [18] Oliven, A.; and Shechter, Y., Extracorporeal photopheresis: a review, *Blood Rev.* **2001**, 15, 103-108.
- [19] Klosner, G.; Trautinger, F.; Knobler, R.; and Neuner, P., Treatment of Peripheral Blood Mononuclear Cells with 8-Methoxypsoralen plus Ultraviolet A Radiation Induces a Shift in Cytokine Expression from a Th1 to a Th2 Response, *J. Invest. Dermatol.* **2001**, 116, 459-462.
- [20] Steen, V. D.; and Medsger, T. A., Improvement in skin thickening in systemic sclerosis associated with improved survival, *Arthritis Rheum.* **2001**, 44, 2828-2835.
- [21] Stern, R. S.; Nichols, K. T.; and Vakeva, L. H., Malignant melanoma in patients treated for psoriasis with methoxsalen (psoralen) and ultraviolet A radiation (PUVA). The PUVA Follow-Up Study, *N. Engl. J. Med.* **1997**, 336, 1041-1045.
- [22] Maier, H.; Schemper, M.; Ortel, B.; Binder, M.; Tanew, A.; and Honigsman, H., Skin Tumors in Photochemotherapy for Psoriasis: A Single-Center Follow-Up of 496 Patients, *Dermatology* **1996**, 193, 185-191.
- [23] Lindelof, B.; Sigurgeirsson, B.; Tegner, E.; Larko, O.; Johannesson, A.; Berne, B.; Ljunggren, B.; Andersson, T.; Molin, L.; Nylander-Lundqvist, E.; and Emtestam, L., PUVA and cancer risk: the Swedish follow-up study, *Br. J. Dermatol.* **1999**, 141, 108-112.
- [24] Luftl, M.; Degitz, K.; Plewig, G.; and Rocken, M., Psoralen Bath Plus UV-A Therapy Possibilities and Limitations, *Arch. Dermatol.* **1997**, 133, 1597-1603.
- [25] Derie, M. A.; Vaneendenburg, J. P.; Versnick, A. C.; Stolk, L. M. L.; Bos, J. D.; and Westerhof, W., A new psoralen-containing gel for topical PUVA therapy: development, and treatment results in patients with palmoplantar and plaque-type psoriasis, and hyperkeratotic eczema, *Br. J. Dermatol.* **1995**, 132, 964-969.
- [26] Grundmann-Kollmann, M.; Behrens, S.; Peter, R. U.; and Kerscher, M., Treatment of severe recalcitrant dermatoses of the palms and soles with PUVA-bath versus PUVA-cream therapy, *Photodermatol. Photoimmunol. Photomed.* **1999**, 15, 87-89.
- [27] Grundmann-Kollmann, M.; Ochsendorf, F.; Zollner, T. M.; Spieth, K.; Kaufmann R.; and Podda, M., Cream PUVA therapy for scleredema adultorum, *Br. J. Dermatol.* **2000**, 142, 1058-1059.
- [28] Von Kobyletzki, G.; Hoffmann, K.; Kerscher, M.; and Altmeyer, P., Plasma levels G. von Kobyletzki, K. Hoffmann, of 8-methoxypsoralen following PUVA-bath photochemotherapy, *Photodermatol. Photoimmunol. Photomed.* **1998**, 14, 136-138.
- [29] Thomas, S. E.; Osullivan, J.; and Balac, N., Plasma levels of 8-methoxypsoralen following oral or bath-water treatment, *Br. J. Dermatol.* **1991**, 125, 56-58.
- [30] Becke, A. D., Density-functional thermochemistry. IV. A new dynamical correlation functional and implications for exact-exchange mixing, *J. Chem. Phys.* **1996**, 104, 1040-1046.
- [31] Cancès, E.; Mennucci, B.; Tomasi, J., A new integral equation formalism for the polarizable continuum model: Theoretical background and applications to isotropic and anisotropic dielectrics. *Journal of Chemical Physics* **1997**, 107, (8), 3032-3041.
- [32] Mennucci, B.; Tomasi, J., Continuum solvation models: A new approach to the problem of solute's charge distribution and cavity boundaries. *Journal of Chemical Physics* **1997**, 106, (12), 5151-5158.
- [33] Cossi, M.; Scalmani, G.; Rega, N.; and Barone, V., New developments in the polarizable continuum model for quantum mechanical and classical calculations on molecules in solution. *J. Chem. Phys.* **2002**, 117, (1), 43-54.
- [34] Gaussian 03, R. B., Frisch, M. J.; Trucks, G. W.; Schlegel, H. B.; Scuseria, G. E.; Robb, M. A.; Cheeseman, J. R.; Montgomery, J. A., Jr.; Vreven, T.; Kudin, K. N.; Burant, J. C.; Millam, J. M.; Iyengar, S. S.; Tomasi, J.; Barone, V.; Mennucci, B.; Cossi, M.; Scalmani, G.; Rega, N.; Petersson, G. A.; Nakatsuji, H.; Hada, M.; Ehara, M.; Toyota, K.; Fukuda, R.; Hasegawa, J.; Ishida, M.; Nakajima, T.; Honda, Y.; Kitao, O.; Nakai, H.; Klene, M.; Li, X.; Knox, J. E.; Hratchian, H. P.; Cross, J. B.; Bakken, V.; Adamo, C.; Jaramillo, J.; Gomperts, R.; Stratmann, R. E.; Yazyev,

O.; Austin, A. J.; Cammi, R.; Pomelli, C.; Ochterski, J. W.; Ayala, P. Y.; Morokuma, K.; Voth, G. A.; Salvador, P.; Dannenberg, J. J.; Zakrzewski, V. G.; Dapprich, S.; Daniels, A. D.; Strain, M. C.; Farkas, O.; Malick, D. K.; Rabuck, A. D.; Raghavachari, K.; Foresman, J. B.; Ortiz, J. V.; Cui, Q.; Baboul, A. G.; Clifford, S.; Cioslowski, J.; Stefanov, B. B.; Liu, G.; Liashenko, A.; Piskorz, P.; Komaromi, I.; Martin, R.

L.; Fox, D. J.; Keith, T.; Al-Laham, M. A.; Peng, C. Y.; Nanayakkara, A.; Challacombe, M.; Gill, P. M. W.; Johnson, B.; Chen, W.; Wong, M. W.; Gonzalez, C.; Pople, J. A. Gaussian, Inc., Wallingford CT, 2004.  
 [35] Lissi, E. A.; Encinas, M. V.; Lemp, E.; Rubio, M. A., Singlet oxygen O<sub>2</sub>(Δg) bimolecular processes – solvent and comparatmentalization effects. *Chemical Reviews* 1993, 93, 699-723.

**Table S1.** Mulliken atomic charges (MPWB95/6-311+G(d,p) level) for selected atoms of singlet (S), radical anion (RA), radical cation (RC), triplet (T), and transition state (TS) of 8MOP of fluorine substitutions, for atomic labeling see Figure-1.

System	C <sub>2</sub>	C <sub>3</sub>	C <sub>4</sub>	C <sub>4</sub>	C <sub>5</sub>	C <sub>6</sub>	C <sub>7</sub>	C <sub>8</sub>	C <sub>9</sub>	C <sub>10</sub>	C <sub>12</sub>	O <sub>13</sub>
X <sub>1</sub> system												
S	0.254	-0.529	0.685	0.545	-----	0.532	-0.778	-0.844	-----	0.960	-0.313	-0.285
RA	0.242	-0.349	-0.396	-----	-----	-----	-----	-----	-2.097	2.522	-0.364	-0.425
RC	0.265	-0.443	0.549	0.691	0.209	0.561	-0.542	-0.878	-1.481	1.236	-----	-----
T	0.243	-----	-0.454	0.579	-----	0.575	-0.424	-0.839	-1.821	1.397	-0.269	-0.285
TS	-0.26	-0.388	-0.388	0.215	-----	1.119	-0.193	-0.870	-2.208	2.257	-0.363	-0.416
X <sub>2</sub> system												
S	0.279	-0.492	0.732	0.791	0.385	0.406	-1.073	-0.818	-1.337	0.898	-0.323	-0.283
RA	0.232	-0.360	-0.299	0.264	-----	1.194	-1.366	-0.907	-2.001	2.311	-0.364	-0.422
RC	0.297	-0.416	0.577	0.954	0.413	0.281	-0.688	-0.891	-1.722	1.292	-0.284	-----
T	0.240	-0.450	0.513	0.861	-----	-----	-0.336	-0.930	-1.723	1.417	-0.268	-0.315
TS	0.313	-0.389	-----	0.338	0.365	1.092	-1.409	-0.809	-2.244	2.297	-0.374	-0.347
X <sub>3</sub> system												
S	0.389	-0.457	-----	-----	-----	1.589	-1.690	-1.047	-2.527	2.882	-0.367	-0.281
RA	0.317	-0.460	-----	-----	-----	1.313	-1.157	-1.131	-2.360	2.582	-0.366	-0.424
RC	0.325	0.574	1.055	0.776	-----	0.398	-0.379	1.071	-1.710	1.361	-0.282	-----
T	0.283	-0.594	1.049	0.650	-0.30	0.412	-----	-1.125	-1.788	1.453	-0.270	-0.323
TS	-----	0.212	-1.468	-----	-----	1.055	-1.197	-0.342	-0.454	1.795	-0.369	-0.344
X <sub>4</sub> system												
S	0.211	-0.289	0.581	0.577	0.213	0.250	-0.629	-0.850	-1.328	1.170	-0.312	-0.291
RA	-----	-----	-0.513	-----	-----	1.256	-1.225	-0.857	-1.863	2.473	-0.364	-0.422
RC	0.214	-0.214	0.481	0.709	0.222	0.205	0.374	-0.876	-1.570	1.417	-0.278	-----
T	-----	-0.239	0.417	0.579	-0.22	-----	-----	-0.898	-1.481	1.447	-0.266	-0.318
TS	0.435	-0.762	0.479	-----	-----	1.406	-1.122	-1.243	-2.169	2.403	-----	-0.343
X <sub>5</sub> system												
S	0.462	-0.616	0.738	0.608	-----	0.430	-0.915	-0.835	-1.202	1.029	-0.310	-0.272
RA	0.386	-0.382	-0.340	-----	-----	1.264	-1.202	-0.902	-1.951	2.455	-0.363	-0.423
RC	0.446	-0.534	0.647	0.752	-----	0.399	-0.655	-0.884	-1.438	1.256	0.279	-----
T	0.387	-0.513	0.572	0.642	-0.25	0.207	-----	-0.943	-1.411	1.332	-0.264	-0.316
TS	-----	0.413	-0.820	-----	0.264	-1.291	1.038	-0.861	-2.022	2.386	-0.366	-0.306



**Table S2.** Atomic spin densities (MPWB95/6-311+G(d,p) level) on selected atoms for the radical anion (RA), radical cation (RC), triplet (T), and transition state (TS) species for flourine substitution for atomic labeling see Figure 1.

System	C <sub>3</sub>	C <sub>4</sub>	C <sub>5</sub>	C <sub>5</sub>	C <sub>7</sub>	C <sub>8</sub>	C <sub>9</sub>	O <sub>13</sub>
X <sub>1</sub> system								
RA	0.193	0.293	0.265	----	0.135	----	----	0.102
RC	----	----	0.250	0.107	----	0.090	0.262	0.100
T	0.252	0.272	0.207	0.125	----	0.095	2.299	0.243
TS	0.198	0.269	0.285	----	0.122	----	----	0.103
X <sub>12</sub> system								
RA	0.178	0.301	0.303	----	0.100	----	----	0.107
RC	----	----	0.262	0.157	----	0.120	0.235	----
T	0.164	0.154	0.676	0.217	----	0.350	----	0.115
TS			0.343	0.107	-0.26	----	----	----
X <sub>3</sub> system								
RA	0.166	0.331	0.255	----	0.108	----	----	0.109
RC	----	----	0.262	----	----	0.169	0.197	----
T	0.205	0.192	0.581	0.127	----	0.343	----	0.107
TS	----	----	0.927	----	----	----	----	----
X <sub>4</sub> system								
RA	0.146	0.259	0.374	----	0.113	----	----	----
RC	----	----	0.282	0.107	0.242	0.125	----	----
T	0.137	0.145	0.737	0.177	----	0.366	0.107	----
TS	-0.123	0.777	0.160	----	----	----	----	----
X <sub>5</sub> system								
RA	0.159	0.308	0.247	----	----	----	----	0.140
RC	----	----	0.302	0.106	----	0.118	0.261	----
T	0.194	0.126	0.726	0.148	----	0.359	----	0.126
TS	0.661	----	----	----	----	----	----	----

**Table S3.** Mulliken atomic charges (MPWB95/6-311+G(d,p) level) for selected atoms of singlet (S), radical anion (RA), radical cation (RC), triplet (T), and transition state (TS) of 8MOP of bromine substitutions, for atomic labeling see Figure-1.

system	C <sub>2</sub>	C <sub>3</sub>	C <sub>4</sub>	C <sub>4</sub>	C <sub>5</sub>	C <sub>6</sub>	C <sub>7</sub>	C <sub>8</sub>	C <sub>9</sub>	C <sub>10</sub>	C <sub>12</sub>	O <sub>13</sub>
X <sub>1</sub> system												
S	0.246	-0.521	0.693	0.671	0.351	0.400	-1.172	-0.930	-1.242	1.105	-0.324	-0.281
RA	0.281	-0.295	-0.415	0.275	0.412	0.908	-1.293	-0.959	-2.500	2.651	-0.365	-0.420
RC	0.262	-0.436	0.579	0.812	0.434	0.426	-1.015	-0.979	-1.562	1.343	-0.287	-0.176
T	0.260	-0.471	0.476	0.757	0.200	0.333	-0.686	-0.992	-1.951	1.583	0.275	-0.306
TS	0.272	-0.390	-0.302	-0.41	----	1.122	-1.505	-0.781	-2.099	2.533	-0.368	-0.377
X <sub>2</sub> system												
S	0.302	-0.470	0.204	0.502	-0.320	1.123	-0.205	-0.987	-2.389	2.037	-0.317	-0.282
RA	0.211	-0.382	-0.331	0.383	-0.240	1.358	-1.235	-1.022	-1.891	2.232	-0.364	-0.420
RC	0.277	-0.348	----	0.575	-0.441	1.175	----	-1.034	-2.304	2-140	-0.287	-0.180
T	0.197	-0.423	----	0.456	-0.771	1.154	----	-1.036	-1.932	1.896	-0.273	-0.314
TS	0.280	-0.359	-0.393	0.450	-0.230	1.259	-0.816	-0.953	-2.217	2.602	-0.374	-0.372
X <sub>3</sub> system												
S	----	-0.329	0.285	0.581	-0.590	0.508	-0.509	-0.662	-0.225	0.857	-0.329	-0.281
RA	----	----	-0.705	0.280	-0.554	0.983	-1.033	-0.953	-1.009	2.597	-0.363	-0.415
RC	----	-0.250	0.259	0.667	-0.601	0.428	-0.269	-0.614	-0.336	0.870	-0.290	-0.186
T	----	-0.315	0.312	0.640	-0.685	0.341	-0.229	-0.670	-0.336	0.792	-0.277	-0.317
TS	0.269	-0.442	-0.459	----	----	0.949	-0.919	-0.962	-0.713	2.579	-0.365	-0.372
X <sub>4</sub> system												
S	0.317	-0.271	1.086	0.578	----	0.278	-0.820	-1.028	-1.435	1.122	-0.319	-0.284

RA	0.228	-0.375	0.907	0.315	-0.491	0.770	-0.474	-1.228	-1.612	1.568	-0.364	-0.413
RC	0.307	-0.231	1.006	0.746	-----	0.220	-0.538	-1.015	-1.600	1.258	-0.281	-0.181
T	0.258	-0.281	0.964	0.653	-0.474	0.257	-0.229	-1.040	-1.777	1.446	-0.267	-0.310
TS	0.231	-0.716	1.110	0.428	-0.202	0.591	-1.060	-0.803	-0.569	0.577	-0.362	-0.382
X5 system												
S	-----	-----	0.723	0.602	0.224	0.720	-1.013	-0.902	-1.564	0.942	-0.316	-0.231
RA	-----	-----	0.666	0.471	-----	0.951	-0.815	-1.152	-1.520	0.898	-0.360	-0.368
RC	-----	-----	0.588	0.787	0.255	0.631	-0.864	-0.882	-1.607	0.993	-0.277	-0.136
T	-----	-----	0.636	0.538	-----	0.784	-0.918	-0.915	-1.766	1.056	-0.359	-0.225
TS	-----	1.033	-1.035	-----	-----	1.076	-1.192	-1.084	-1.954	2.442	-0.364	-0.285

**Table S4.** Atomic spin densities (MPWB95/6-311+G(d,p) level) on selected atoms for the radical anion (RA), radical cation (RC), triplet (T), and transition state (TS) species for bromine substitution for atomic labeling see Figure 1.

system	O <sub>1</sub>	C <sub>3</sub>	C <sub>4</sub>	C <sub>5</sub>	C <sub>5</sub>	C <sub>8</sub>	C <sub>9</sub>	O <sub>13</sub>
X <sub>1</sub> system								
RA	-----	0.184	0.285	0.294	-----	-----	-----	0.105
RC	0.107	-----	-----	0.255	0.110	-----	0.255	-----
T	0.170	0.159	0.246	0.442	0.160	0.239	-----	-----
TS	-----	-----	-----	0.287	0.251	-----	-----	-----
X <sub>2</sub> system								
RA	-----	0.176	0.296	0.303	-----	-----	-----	0.106
RC	0.105	-----	-----	0.256	0.153	-----	0.229	-----
T	0.105	0.162	0.159	0.652	0.219	0.347	0.107	0.119
TS	-----	-----	0.108	-----	0.109	-----	-----	-----
X <sub>3</sub> system								
RA	-----	0.195	0.251	0.259	-----	-----	-----	0.104
RC	-----	-----	-----	0.257	-----	0.153	0.203	-----
T	-----	0.200	0.122	0.605	0.158	0.363	-----	-----
TS	-----	-----	-----	0.545	-----	-----	-----	-----
X <sub>4</sub> system								
RA	-----	0.219	0.262	0.286	-----	-----	-----	0.101
RC	0.108	-----	-----	0.281	0.109	0.123	0.249	-----
T	0.142	0.180	0.200	0.554	0.168	0.284	0.170	0.143
TS	-----	-----	0.493	-----	-----	-----	-----	-----
X <sub>5</sub> system								
RA	-----	0.132	0.394	0.261	-----	-----	-----	0.108
RC	0.103	-----	-----	0.288	0.110	0.124	0.254	-----
T	-----	0.590	0.534	0.362	-----	-0.10	0.124	0.231
TS	-----	0.599	-----	-----	-----	-----	-----	-----